

Polyanionic, Alkylthiosulfate-Based Thiol Precursors for Conjugated Polymer Self-Assembly onto Gold and Silver

Mario Kraft,[†] Sylwia Adamczyk,[†] Andreas Polywka,[‡] Kirill Zilberberg,[‡] Christ Weijters,[§] Jens Meyer,[§] Patrick Görrn,[‡] Thomas Riedl,[‡] and Ullrich Scherf^{*,†}

[†]Bergische Universität Wuppertal, Macromolecular Chemistry Group (buwmakro) and Institut für Polymertechnik (IfP), Gauss-Strasse 20, D-42119 Wuppertal, Germany

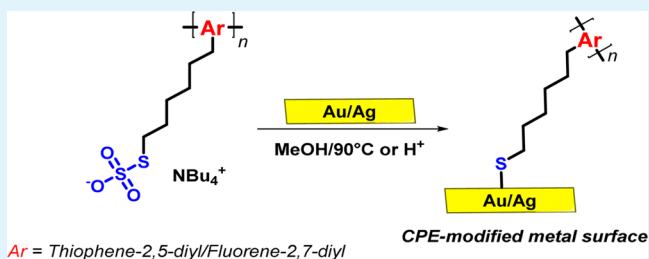
[‡]Bergische Universität Wuppertal, Lehrstuhl für Elektronische Bauelemente and Institut für Polymertechnik (IfP), Rainer-Gruenter-Strasse 21, D-42119 Wuppertal, Germany

[§]Philips Research, Philipsstrasse 8, 52068 Aachen, Germany

S Supporting Information

ABSTRACT: Anionic, conjugated thiophene- and fluorene-based polyelectrolytes with alkylthiosulfate side chains undergo hydrolysis under formation of alkylthiol and dialkyldisulfide functions. The hydrolysis products can be deposited onto gold or silver surfaces by self-assembly from solutions of the anionic conjugated polyelectrolyte (CPE) precursors in polar solvents such as methanol. This procedure allows solution-based surface modifications of gold and silver electrodes using environmentally friendly solvents and enables the formation of conjugated polymer bilayers. The herein presented alkylthiosulfate-substituted CPEs are promising candidates for increasing the work function of gold and silver electrodes thus improving hole injection from such electrode assemblies into organic semiconductors.

KEYWORDS: conjugated polyelectrolytes (CPE), Bunte salts, self-assembly, cross-linking, charge injection interlayer, conjugated polymer bilayer

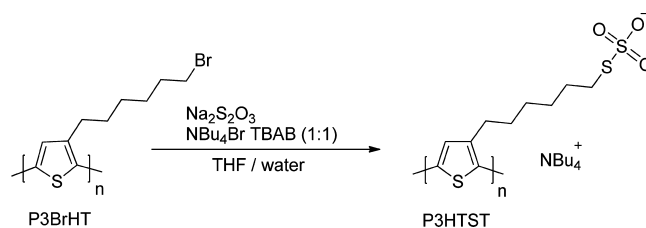


Ar = Thiophene-2,5-diyl/Fluorene-2,7-diyl

INTRODUCTION

Deposition of thin organic surface layers (so-called self-assembled monolayers, SAMs) of thiols onto gold is a well-established procedure of nanotechnology resulting in surface modification and functionalization for various applications in (bio)chemistry, sensing technology, and organic electronics.¹ Hereby, the SAM procedure allows for the attachment of functional surface moieties as recognition units for specific analytes.² Moreover, it allows for a specific modification of the physical and electronic properties of the metal surface, such as wettability, surface tension, absorbance, and electronic work function.^{3–5} In most cases the surface modifiers are attached starting from moderately polar organic molecules as thiol source (free thiols, disulfides, thioesters)⁶ that are soluble in common organic solvents: chlorinated hydrocarbons, aromatic solvents, ethers as tetrahydrofuran or dioxane, etc. For many applications, especially for surface modification of metals, the use of polar solvents such as methanol or water can be highly favorable. Herein, we present the synthesis of regioregular, 3-substituted polythiophenes and 9,9-disubstituted polyfluorenes with alkylthiosulfate side chains, so-called polymeric Bunte salts, carrying tetraalkylammonium counterions (Scheme 1). The thiosulfate functions of the side chains can be converted into alkylthiol (or during further conversion, into dialkyldisulfide) functions simply by heating or/and acidifying the initial

Scheme 1. Synthesis of a Hexylthiosulfate-Functionalized Regioregular Polythiophene-Based Polyelectrolyte P3HTST



solutions in polar solvents or solvent mixtures. The resulting thiol functions of the conjugated polymers are able to self-assemble onto gold or silver surfaces. Moreover, our new scheme also enables the generation of bilayers by depositing a second organic layer from a solution in nonpolar solvents on top of the self-assembled polythiophene or polyfluorene layer.

RESULTS AND DISCUSSION

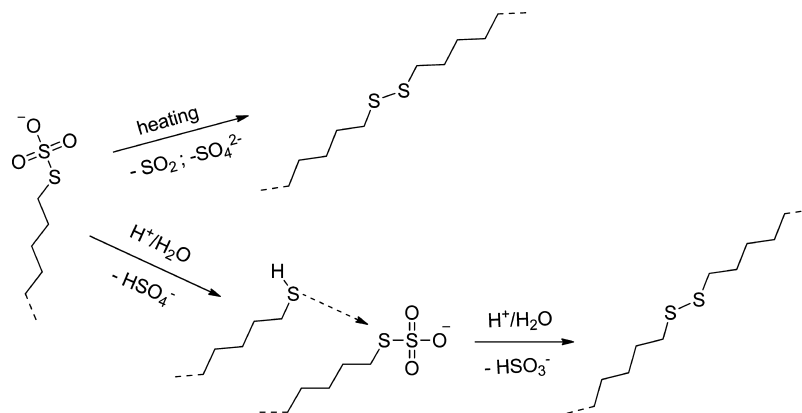
Polythiophene-Based Systems. The synthesis of the polythiophene-based Bunte-type salts starts from the well-

Received: April 25, 2014

Accepted: July 4, 2014

Published: July 4, 2014

Scheme 2. Possible Reactions of the Alkylthiosulfate Side Chains of P3HTST during Hydrolysis/Cross-Linking



known poly(3-bromohexyl)thiophene P3BrHT.^{7,8} Hereby, the synthesis of the P3BrHT precursor follows the guidelines first described by McCullough and co-workers.⁹ Polymer-analogous modification of P3BrHT¹⁰ with a 10-fold excess of a 1:1 w/w mixture of sodium thiosulfate and tetrabutylammonium bromide in a two-phase THF/water mixture leads to the corresponding Bunte-type conjugated polyelectrolyte (CPE) poly(3-thiosulfatohexylthiophene) P3HTST in nearly quantitative yield. Hereby, the bulky tetrabutylammonium counterions enable increased solubility and a, most probably steric, stabilization of the rather reactive and sensitive alkylthiosulfate functions. Attempts to synthesize the corresponding CPE with sodium counterions resulted in insoluble products. Model Bunte salts with simple hexyl side chains not bound to a polythiophene skeleton were also synthesized for an investigation of the influence of the counterion on the thermal stability (see Supporting Information, Figures S5–S7).

The conjugated polyelectrolyte P3HTST was isolated by precipitation, the remaining solvent removed under reduced pressure, and the product dried under high vacuum conditions. The quantitative formation of the thiosulfate-based polyelectrolyte P3HTST can be monitored by NMR spectroscopy, see the Experimental part, and by elemental analysis. The ¹H NMR spectrum of P3HTST (Supporting Information, Figure S1) measured in deuterated methanol-*d*₄ displays typical chemical shifts of the alkyl chains of CPE and counterion in the range of 1.0–3.3 ppm. The methylene signal of the hydrogens next to the thiosulfate group appears at 3.1, the signal of the aromatic thiophene hydrogen at 7.1 ppm. The lowered carbon value of the elemental analysis points to the presence of remaining solvent (water or methanol). Two different P3BrHT batches have been used in our experiments, with number-average molecular weights *M_n* of (A) 3730 and (B) 7890 g/mol. The resulting thiosulfate-substituted polythiophene samples showed fully reversible glass transitions during DSC analysis, the P3HTST batch made from the low *M_n* precursor (A), a glass transition peaking at 18 °C, the higher *M_n* polyelectrolyte (B) at 25 °C, thus indicating the presence of soft products at room temperature (Supporting Information, Figures S2/S3). Other than the slight difference in their thermal behavior, we did not observe significant differences between both batches concerning their self-assembly properties. The formation of the alkylthiosulfate-functionalized conjugated polyelectrolytes is also documented in the occurrence of characteristic IR vibrations for the $\text{RS}_2\text{O}_3\text{-}$ group at 1209, 1020, and 621 cm^{-1} (Supporting Information, Figure S12) and in a character-

istically altered solubility behavior with good solubility in polar solvents such as methanol, ethanol, or acetone.

Hydrolysis of Bunte-type salts (alkylthiosulfates) by heating or/and treatment with diluted acids was described in the literature in detail. The hydrolysis first leads to the formation of free thiol functions under elimination of hydrogensulfate anions (Scheme 2).^{11–14} The as-formed thiol function can further react with another alkylthiosulfate under formation of dialkyldisulfide species and hydrogensulfite anions.¹⁵ The second bimolecular reaction can cause cross-linking under formation of disulfide bridges if our (or other) polyelectrolytes with multiple alkylthiosulfate side chains are hydrolyzed.

Under neutral conditions, hydrolysis of P3HTST takes place at elevated temperature as tested for polyelectrolyte solutions in water/methanol mixtures at 90 °C. For solid state samples, (i) cross-linking should be favored due to a high local concentration of side chains, and (ii) hydrolysis already starts when the samples are exposed to humid air. If films of the novel conjugated polyelectrolyte P3HTST are exposed to air, hydrolysis/cross-linking turns the initially soft, smeary film ($T_g < \text{RT}$) into a cross-linked material with brittle consistence after 12–24 h. Thicker, solid particles undergo incomplete cross-linking preferentially occurring at a surface layer under formation of core–shell particles with a cross-linked shell and a soft core (Supporting Information, Figure S4). Exposure to aqueous HCl fumes distinctly speeds up cross-linking.

UV–vis absorption and photoluminescence (PL) spectra of P3BrHT and P3HTST solutions in chloroform or methanol, respectively, and of corresponding films are depicted in Figure 1 as well as the solid state absorption spectrum of a hydrolyzed, cross-linked P3HTST (h-P3HTST) film after exposure to humid HCl fumes. The solution absorption spectra of P3BrHT and P3HTST are very similar to absorption maxima at 448 and 444 nm, respectively, thus indicating only minor conformational changes during conversion of the neutral P3BrHT precursor into the thiosulfate-substituted CPE. Also the solid state absorption spectra differ only slightly with a more distinct low energy shoulder at ca. 580 nm for the neutral precursor P3BrHT that is indicative of polythiophene aggregation.¹⁶ After cross-linking, the absorption maximum of the resulting network is moderately red-shifted by 23 nm (P3HTST: 513 nm, h-P3HTST: 536 nm) if compared to the linear, thiosulfate-based CPE most probably due to increased interchain interactions.¹⁷ This is also documented by a visible color change of the film from red to violet. Similar trends are observed for the PL spectra. Please note that the PL intensity for P3HTST films is

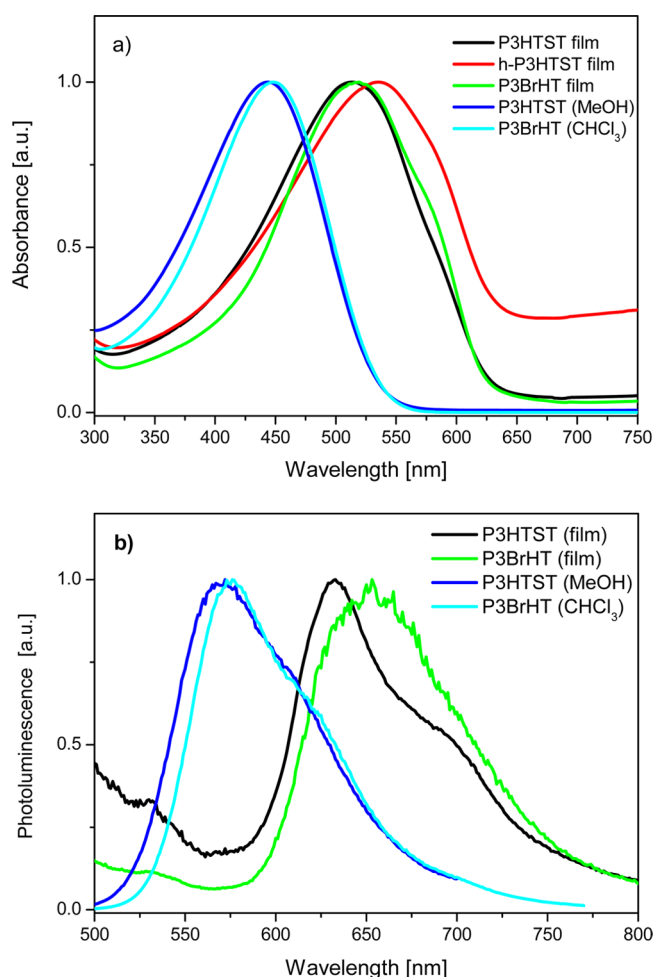


Figure 1. UV-vis absorption (a) and photoluminescence (b) spectra of P3BrHT and P3HTST (batch B) in chloroform (P3BrHT) or methanol (P3HTST) solution, respectively, and as solid films, as well as the solid state absorption spectrum of a cross-linked h-P3HTST film after hydrolysis.

significantly increased if compared to films of the P3BrHT precursor. However, the solid state PL intensity of P3HTST is significantly reduced after cross-linking into h-P3HTST most

probably due to enhanced interchain PL quenching in the resulting polymer network. A weaker absorption band at wavelengths of >650 nm for the cross-linked h-P3HTST film may indicate some self-doping by atmospheric oxygen.¹⁸ Exposure of an h-P3HTST layer to gaseous hydrazine causes virtually complete disappearance of the long-wavelength absorption feature.

Next we investigated the self-assembly of (partially) hydrolyzed h-P3HTST on freshly prepared gold or silver surfaces. Hereby, we treated the gold surfaces with solutions of P3HTST either in acidified methanol at room temperature or in a water/MeOH mix at 90 °C. The surface morphology before and after self-assembling a thin polymer layer onto gold was investigated by AFM microscopy. The deposition of the h-P3HTST surface layer from a solution of the P3HTST precursor in the neutral water/MeOH mix at 90 °C is coupled to an only very slight increase in the average surface roughness from 1.22 to approximately 1.55 nm (Figure 2). The thickness of the self-assembled layers was estimated to be 5 – 30 nm as a function of the contact time between metal surface and CPE solution (see Supporting Information, Table S1) without any significant influence on film roughness. For monitoring the deposition process, we investigated a thin film of h-P3HTST on gold by XPS spectroscopy (S 2p signals).¹⁹ The sample showed the expected S 2p signatures for $-S-Au$ (surface bound CPE chains), $-S-H$ (free thiol), $-S-S-$ (cross-links), and SO_x (Supporting Information, Figure S16). The SO_x species should result from the hydrolysis of thiosulfate functions (see Scheme 2).

UV/vis measurements of as-deposited, thin conjugated polymer layers onto gold show (weak) UV/vis absorption bands peaking at ca. 490 nm, hence located between the absorption maxima of P3HTST solutions (λ_{max} : 444 nm) and films (P3HTST λ_{max} : 513 nm; h-P3HTST λ_{max} : 536 nm).

As reference and as measured by atmospheric pressure photoelectron spectroscopy (AC2 method²⁰), the ionization potential of a spin-coated P3HTST film on ITO was first estimated to be 5.12 eV (4.75 eV for the ITO layer before deposition). Storage of these films under ambient conditions leads to a further increase of the ionization potential up to 5.7 eV, possibly related to the already discussed self-doping of the P3HTST coating by atmospheric oxygen. AC2 analyses of gold

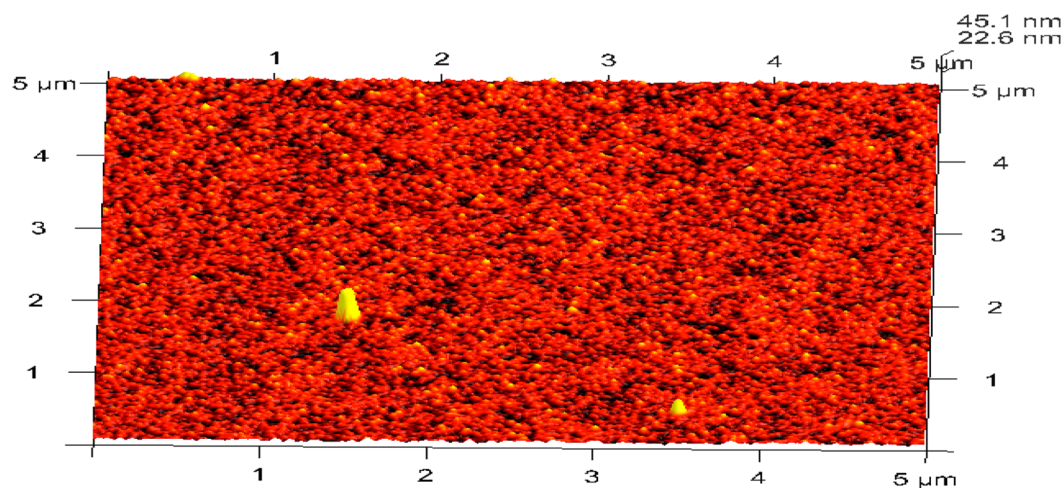
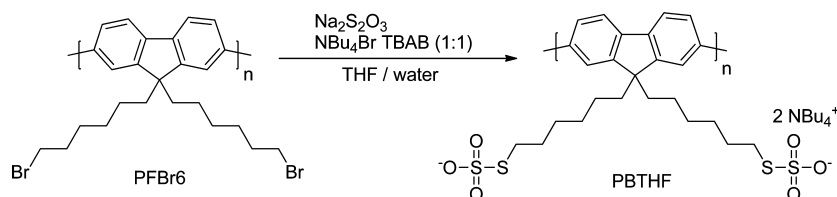


Figure 2. AFM height image of a $5 \times 5 \mu\text{m}^2$ square of hydrolyzed h-P3HTST onto gold, deposited from a solution of the P3HTST precursor in water/methanol at 90 °C (c : 0.1 mg/mL); layer thickness: ca. 20 nm).

Scheme 3. Synthesis of a Hexylthiosulfate-Functionalized Polyfluorene-Based Polyelectrolyte PBTHF



films before (pure Au surface) and after deposition of a thin h-P3HTST layer (ca. 20 nm) from a solution of the P3HTST precursor in either acidified methanol at RT or neutral water/methanol at elevated temperature, respectively, showed a significantly increased ionization potential of the surface-modified gold film (5.30 or 5.15 after vs 4.80 eV before deposition, respectively). In a control experiment the bare gold surface was treated with water/methanol at 90 °C (without addition of P3HTST). This treatment leads to a significantly increased average surface roughness of 3.4 nm. However, the ionization potential is only slightly increased from 4.80 to 4.90 eV. The increased ionization potentials of spin-coated P3HTST films onto ITO (5.12 eV) and self-assembled, (partially) hydrolyzed h-P3HTST (5.30/5.15 eV) onto gold indicate that the ionization potential is mainly determined by the deposited polymer (P3HTST or h-P3HTST, respectively) coating and thus provide evidence for successful surface modification.

Polyfluorene-Based Systems. Based on our findings on polythiophene-based Bunte salts, we next tried to extend our approach to polyfluorene-based systems. Polymer-analogous modification of the well-known poly[9,9-bis(6-bromohexyl)fluorene] PFBBr6 precursor (M_n : 14 300; M_w : 28 500)^{21,22} with a mixture of sodium thiosulfate and tetrabutylammonium bromide in a two-phase THF/water mixture leads to the corresponding Bunte-type conjugated polyelectrolyte (CPE) poly[9,9-bis(3-thiosulfatohexyl)fluorene] PBTHF in very good yield (Scheme 3). The polyfluorene-based CPE shows a drastically altered solubility if compared to the PFBBr6 precursor and is now soluble in polar organic solvents as methanol, DMF, and DMSO. The formation of the thiosulfate-based polyelectrolyte PBTHF was confirmed by ¹H NMR spectroscopy and by an exactly matching elemental analysis (see Experimental section). The ¹H NMR spectrum of PBTHF in methanol-*d*₄ (Supporting Information, Figure S13) shows the expected signals of the tetrabutylammonium counterion, as also observed for P3HTST. The methylene signal of the hydrogens next to the thiosulfate group appears at 3.0 ppm. The resulting 9,9-dialkylthiosulfate-substituted polyfluorene sample showed a weak glass transition at ca. 59 °C during DSC analysis (Supporting Information, Figure S14).

The polyfluorene-based absorption and photoluminescence emission features are quite insensitive to the substitution pattern and weakly sensitive to the aggregation state, as extensively described in the literature.^{23,24} Transition from solution to the solid state only causes a moderate red-shift of the absorption edge (Figure 3a) and a 10–15 nm red-shift of the PL features (Figure 3b), as known for polyfluorenes without β -phase formation. Therefore, the solid state absorption and PL spectra of PFBBr6, PBTHF, and hydrolyzed h-PBTHF are quite similar, as depicted in Figure 3.

As already described for the polythiophene-based P3HTST, also (partially) hydrolyzed h-PBTHF self-assembles on freshly prepared gold (or silver) surfaces. In contrary to P3HTST the self-assembly procedure does not work under neutral

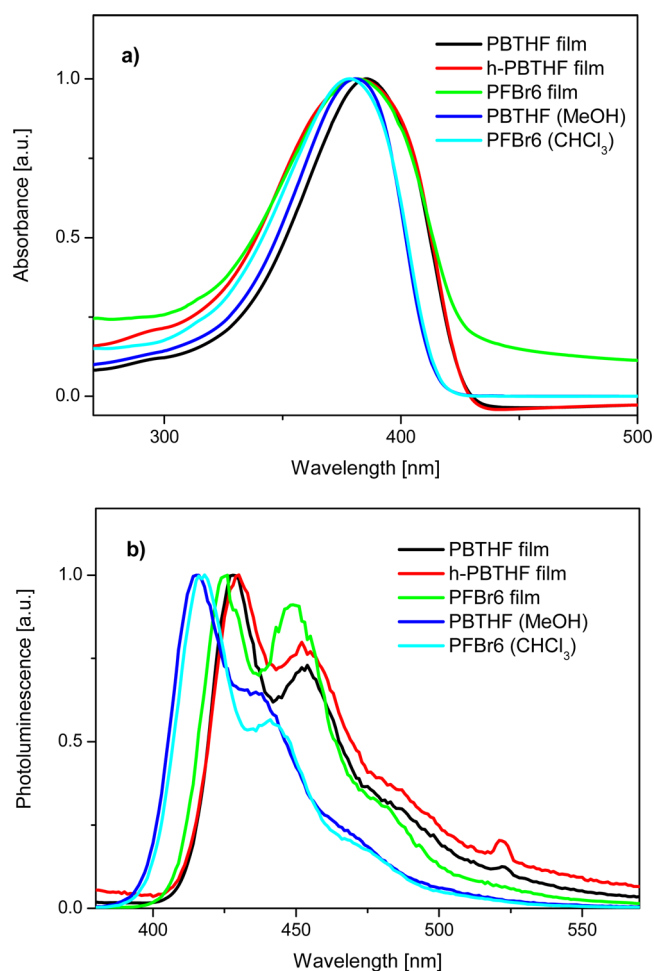


Figure 3. UV–vis absorption (a) and photoluminescence (b) spectra of PFBBr6 and PBTHF in chloroform (PFBBr6) or methanol (PBTHF) solution and as solid films, as well as the solid state absorption and PL spectra of a cross-linked h-PBTHF film after hydrolysis (the weak PL band at ca. 525 nm is an artifact).

conditions for PBTHF. For polymer self-assembly we treated the gold surfaces with a CPE solution in acidified methanol for 5–20 h. The surface morphology after self-assembling the PBTHF layer was next investigated by AFM (see Figure 4). The deposition of the surface layer is coupled to a slight decrease in the average surface roughness from 1.22 to 1.0 nm. The thickness of the thin h-PBTHF layer depends on the contact time and was ca. 10 nm for a contact time of 6 h (Supporting Information, Table S1). The XPS S 2p spectrum of a thin h-PBTHF film on gold showed signatures for –S–Au (surface bound CPE chains), –S–H (free thiol), –S–S– (cross-links), and SO_x as already described for the polythiophene-based CPE (Supporting Information, Figure S16).

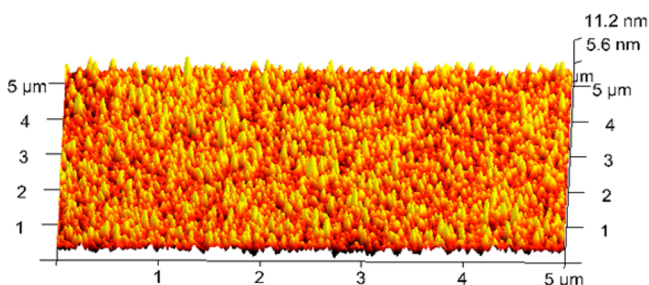


Figure 4. AFM height image of a $5 \times 5 \mu\text{m}^2$ square of hydrolyzed h-PBTHF onto gold, deposited from a solution of the PBTHF precursor in acidified methanol (conc.: one drop conc. aqueous HCl/10 mL MeOH).

UV/vis and fluorescence measurements of as-deposited, thin h-PBTHF layers onto silver and gold (thickness ca. 20 nm) show the typical UV/vis absorption feature related to polyfluorenes peaking at ca. 380 nm as shown for deposition onto silver in Figure 5a. Excitation of the films at 350 or 360 nm causes PL spectra that are quite similar to those of a spin-coated PBTHF film on ITO (Figure 5b). These absorption and PL signatures are a clear proof for the presence of the self-assembled h-PBTHF layer.

AC2 analyses of Au samples before and after h-PBTHF deposition from a solution of the CPE precursor in acidified

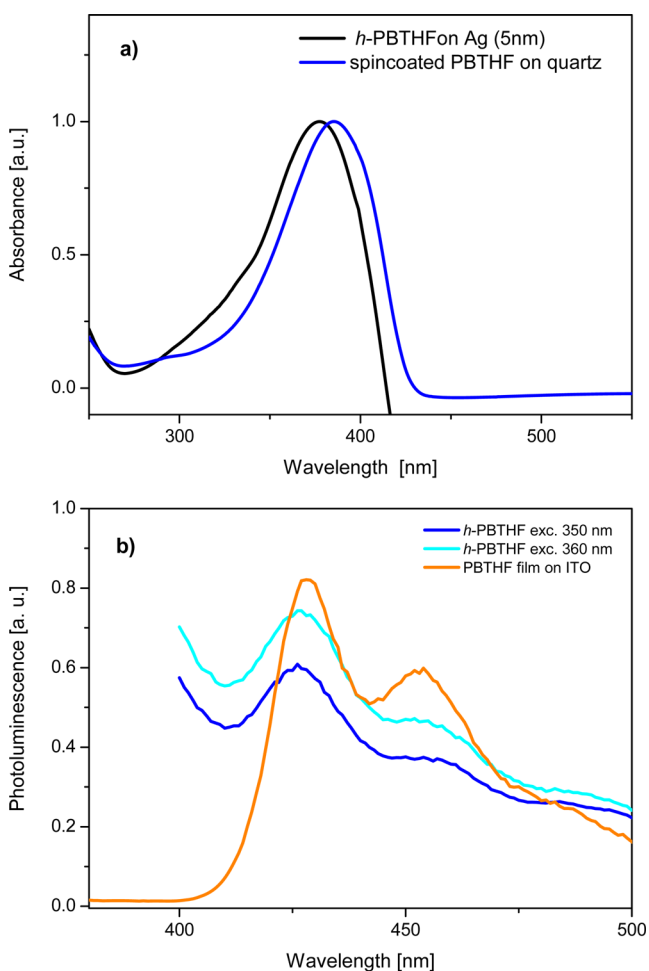


Figure 5. UV–vis absorption (a) and photoluminescence (b) spectra of self-assembled h-PBTHF on silver and spin-coated PBTHF on ITO.

methanol showed a significantly increased ionization potential of the surface-modified gold film (5.80 after vs 4.80 eV before deposition, respectively), thus providing further evidence for the expected surface modification. For silver, the ionization potential increases from 4.65 eV (before) to 5.55 eV (after deposition). For comparison, a spin-coated PBTHF film onto ITO displayed an ionization potential of 5.6 eV.

Bilayer Formation. Finally, we have tested the possibility for bilayer formation onto silver applying the orthogonal solubility principle. Toward this end, we have deposited a second layer of poly(carbazole-*alt*-dithienylbenzothiadiazole) PCDTBT²⁵ by spin-coating from chloroform on top of a thin, self-assembled layer of hydrolyzed h-PBTHF. PCDTBT was selected because of its HOMO level at ca. 5.5 eV,²⁶ near the ionization potential of the h-PBTHF-modified silver surface/electrode. The absorption spectra of a h-PBTHF/PCDTBT bilayer is depicted in Figure 6. The UV–vis spectrum of the bilayer is clearly a superposition of the absorption spectra of both components.

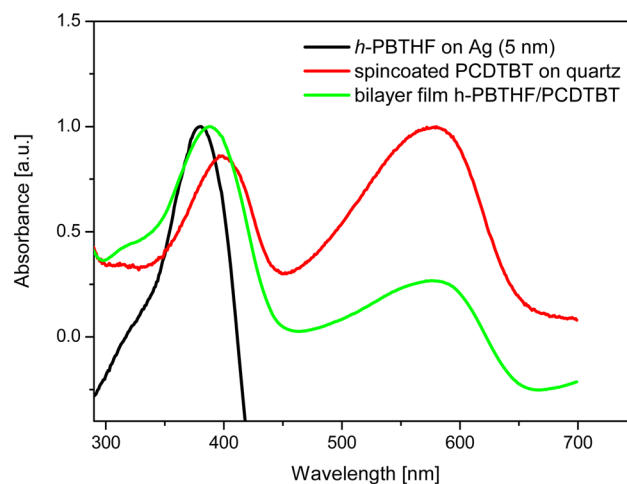


Figure 6. Solid state absorption spectra of a bilayer film h-PBTHF/PCDTBT on silver. Baseline correction for the polymer layers on silver is dissatisfying.

Hole-Only Devices. To study the possible application of the self-assembled layer of hydrolyzed PBTHF as anode interlayer for organic electronic devices, we prepared hole-only test structures with a layer sequence glass/Cr/Au (with or without h-PBTHF)/PCDTBT/MoO₃/Ag (Figure 7a). Details about device fabrication can be found in the Experimental section. Due to its extraordinarily high work function (WF) of 6.7 eV, MoO₃ forms a favorable hole injecting interface even to organic semiconductors with very deep HOMO levels.^{27,28} At the same time, electron injection via MoO₃ can be neglected in our hole-only devices. The corresponding *I/V* characteristics in forward and reverse direction are shown in Figure 7b. In reverse direction the MoO₃ layer is positively biased, and, consequently, efficient hole injection via MoO₃ is observed for all devices.

In forward direction substantial variations in the injected hole current are clearly seen. For the device with a neat Au anode, a very low hole current (about 2×10^{-7} A @ 2 V) is observed. Note, at -2 V (reverse direction), the injected hole current via MoO₃ is more than 3 orders of magnitude higher. This can be understood by the unfavorably large energetic mismatch of the Fermi level of Au (WF: 4.8 eV) and the relatively deep lying

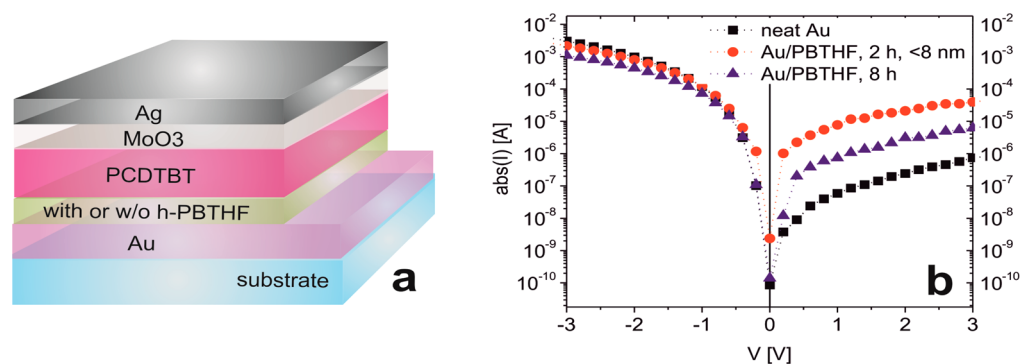


Figure 7. (a) Layer sequence of the hole-only devices comprising either a neat or a PBTHF-modified Au electrode. (b) I/V characteristics of the respective devices. The forward direction (positive voltage) is defined for the Au electrode being the anode.

HOMO level reported for PCDTBT (ca. 5.5 eV)^{26,29} and the resulting energetic barrier for hole injection. This is in agreement with a report by Seo et al., who determined a barrier for hole injection of 0.7 eV at the Au/PCDTBT interface.³⁰ As depicted in Figure 7b, the hole injection improves substantially if the Au electrode is coated with a thin layer of h-PBTHF. As evidenced by the Kelvin probe method, coating the Au electrode with a thin h-PBTHF layer of less than 8 nm increases the WF by roughly 200 meV. In the I/V characteristics, this leads to an almost 2 orders of magnitude higher hole current, as a result of a lowered hole-injection barrier. Apparently, the thickness of the h-PBTHF interlayer plays an important role, as for the thicker h-PBTHF layer a significant drop in current is found (also in reverse direction, Figure 7b). This decrease can be attributed to an increased series resistance with increasing thickness of the interlayer, thus favoring the use of thin h-PBTHF interlayers for interface modification. Even though the injected hole current via the modified Au electrode is still noticeably smaller than that via an evaporated MoO₃ interlayer at the same bias level, the results of these first experiments are very encouraging and raise hope that a further improvement can be achieved.

CONCLUSION

In conclusion, we have developed a straightforward synthetic procedure toward 3-hexylthiosulfate-substituted, regioregular polythiophene (P3HTST) and polyfluorene (PBTHF) derivatives carrying tetrabutylammonium counterions. We could demonstrate the hydrolysis of P3HTST and PBTHF into conjugated polythiophenes h-P3HTST and polyfluorenes h-PBTHF carrying alkylthiol functions. The alkylthiol side chains that are formed during hydrolysis are used as anchoring groups for polymer self-assembly onto gold or silver surfaces starting from P3HTST and PBTHF solutions in environmentally friendly, polar solvents such as methanol. The presence of a large number of anchoring groups of the multifunctional polyelectrolyte guarantees a robust coverage of the underlying metal electrodes in a simple wet-processing procedure.³¹ Solid state hydrolysis leads to formation of dialkyldisulfide cross-links in a bimolecular reaction between as-formed alkylthiol and neighboring alkylthiosulfate functions. The new scheme allows for the preparation of conjugated polymer bilayer stacks. Hole-only devices with PBTHF-modified gold electrodes and poly(carbazole-*alt*-dithienylbenzothiadiazole) PCDTBT as polymeric semiconductor demonstrated an increase of the hole current by 2 orders of magnitude compared to devices based on nonmodified gold electrodes. This is attributed to an increase of

the work function of the Au electrode and a concomitant reduction of the hole injection barrier at the Au/PCDTBT interface.

EXPERIMENTAL PROCEDURES

3-Bromoethyl-substituted polythiophene P3BrHT was prepared following a procedure that has been developed by McCullough and co-workers.⁹ 9,9-Bis(6-bromoethyl)-substituted polyfluorene PFB6 was synthesized in a Suzuki cross-coupling of the AB-type monomer 2-tetramethyldioxaborolane-7-bromo-9,9-bis(6-bromoethyl)fluorene. The model compound sodium *S*-hexylthiosulfate was made as already described.¹⁰ The synthesis of the second model compound (tetra-*n*-butylammonium *S*-hexylthiosulfate) is described in the Supporting Information (Scheme S2).

P3HTST. One hundred sixty milligrams (0.65 mmol units) of Br-P3HT (M_n : 7890; M_w : 8470 g/mol), 1.4 g (4.3 mmol) of tetra-*n*-butylammonium bromide (TBAB), and 1.4 g (8.9 mmol) of sodium thiosulfate were placed under inert gas conditions into a Schlenk tube. Fifteen milliliters of dry THF and 2 mL of water were added. The resulting two-phase mixture was stirred at 80 °C overnight. The organic phase was dialyzed, first against methanol/water (1/1, v/v) and second against pure methanol. After dialysis the conjugated polyelectrolyte was precipitated into diethyl ether. The soft product still contains methanol. Next, the solvent was removed under reduced pressure, and the product dried under high vacuum conditions. The resulting 324 mg of P3HTST (yield: 96%) as hygroscopic solid is stored under inert conditions.

¹H NMR (400 MHz, CD₃OD): δ 7.05 (s, 1 H), 3.24 (m, 8 H), 3.10 (m, 2 H), 2.85 (m, 2 H), 1.83–1.75 (m, 4 H), 1.67 (m, 8 H), 1.53 (m, 4 H), 1.45 (m, 8 H), 1.03 (t, $J = 7.3$ Hz, 12 H).

¹³C NMR (400 MHz, CD₃OD): δ 141.0, 134.9, 131.6, 129.5, 59.6, 36.2, 31.7, 31.0, 31.0, 30.6, 30.1, 30.0, 24.9, 20.8, 14.2.

Elemental analysis: (C₂₆H₄₉NO₃S₃)_{*n*}, calcd (%): C 60.07, H 9.50, N 2.69, S 18.50, measured (%): C 56.52, H 9.01, N 2.17, S 18.08.

TGA: first decomposition step 222 °C (14.7%); second decomposition step 290 °C (39.2%).

DSC: $T_g = 25$ °C.

PFB6. One gram of 2-tetramethyldioxaborolane-7-bromo-9,9-bis(bromoethyl)fluorene and 30 mg of Pd(PPh₃)₄ were dissolved in 5 mL of a 2 M aqueous Na₂CO₃ solution and 7 mL of toluene. The mixture was heated to 60 °C for 12 h. Three milliliters of a 0.1 M solution of bromobenzene in toluene as end-capper was finally added, and the mixture reacted for further 2 h. The polymer was precipitated into methanol and purified by solvent extraction with methanol, acetone, ethyl acetate, and dichloromethane. Finally, the dichloromethane fraction was concentrated by evaporation and reprecipitated into methanol. After drying, 421 mg (60%) of a slightly yellow solid is isolated.

¹H NMR (400 MHz, C₂D₂Cl₄): 7.87–7.39 (m, 6 H), 3.33 (m, 4 H), 2.15 (m, 4H), 1.72 (m, 4 H), 1.29–1.19 (m, 8 H), 0.87 (m, 4 H).

¹³C NMR (400 MHz, C₂D₂Cl₄): δ 151.8, 140.4, 140.3, 126.4, 121.6, 120.5, 55.5, 40.3, 34.8, 32.9, 29.4, 28.1, 24.1.

M_n : 14 300; M_w : 28 500.

PBTHF. Two hundred milligrams (0.41 mmol, of repeat units) of PFBBr₆, 2.2 g (6.82 mmol) of tetra-*n*-butylammonium bromide (TBAB), and 2.3 g (14.55 mmol) of sodium thiosulfate were dissolved in a mix of 20 mL of THF and 6 mL of water. The solution was stirred at 80 °C under inert gas conditions overnight. The organic phase of the two-phase mixture was isolated and the solvent removed under reduced pressure. The slimy residue was dispersed into 200 mL of water and stirred for 10 min. The resulting white solid was isolated by filtration and dried under vacuum overnight. Next the product was treated with hexane and dichloromethane by Soxhlet extraction. The dichloromethane phase was isolated and the solvent removed by evaporation. The resulting residue was again dispersed into water. Filtration and drying of the resulting solid product gave 227 mg (yield: 51%) of a slightly yellow solid.

¹H NMR (400 MHz, CD₃OD): δ 7.97–7.37 (m, 6 H), 3.23 (m, 16 H), 3.01 (m, 4 H), 2.25 (m, 4H), 1.65 (m, 20 H), 1.45–1.13 (m, 28 H), 1.01 (t, *J* = 7.4 Hz, 12 H).

¹³C NMR (400 MHz, CD₃OD): δ 152.9, 142.03, 141.6, 127.6, 122.5, 121.4, 59.6, 56.6, 41.4, 36.0, 31.9, 30.5, 29.7, 25.3, 24.9, 20.7, 14.1.

Elemental analysis: (C₅₇H₁₀₂N₂O₆S₄)_{*n*} calcd (%): C 65.85, H 9.89, N 2.69, S 12.34, measured (%): C 65.42, H 10.27, N 2.60, S 12.13.

TGA: first decomposition step 250 °C (9.2%); second decomposition step 282 °C (43.8%).

DSC: $T_g = 59$ °C.

Assembly of Hydrolyzed h-P3HTST and h-PBTHF onto Gold.

(A) Acid-free conditions: A freshly prepared gold film onto quartz was treated with 20 mL of a dilute (0.2 mM) solution of P3HTST in methanol/water (v/v 3/1) for 15 h at 90 °C. Next the gold film was rinsed three times with methanol and air-dried.

(B) Acidic conditions: A freshly prepared gold film was treated with 10 mL of an acidified (addition of 20 μL of concentrated hydrochloric acid) solution of 1 mg P3HTST or PBTHF in 10 mL of methanol for 1–40 h at room temperature. Next the gold film was rinsed three times with methanol and air-dried.

Hole-Only Devices. Hole-only devices with the following layer sequence have been prepared: glass/Cr 2 nm/Au 80 nm/h-PBTHF/PCDTBT 120 nm/MoO₃ 40 nm/Ag 150 nm. The active device area was 3.14 mm² as defined by photolithography. Cr, Au, MoO₃, and Ag were thermally evaporated at base pressure of 10⁻⁶ mbar. Cr was used as adhesion promoter. For interlayer deposition the metal films were stored in methanol for 15 h. Subsequently they were transferred into a solution of 1 mg of PBTHF in 10 mL of methanol/20 μL of concentrated, aqueous hydrochloric acid. After 2 or 8 h at room temperature, they were finally rinsed with methanol and vacuum-dried. PCDTBT was spin-casted under inert atmosphere using a filtered (0.45 μm PTFE filter) chlorobenzene solution that has been stirred overnight at 80 °C under N₂. The polymer layer was consequently dried at 70 °C for 5 min under N₂. The work function of neat and surface-modified gold was measured with a McAllister KP6500 K-Probe system in ambient air. Highly ordered pyrolytic graphite with a WF of 4.5 eV was used as reference.^{32,33}

■ ASSOCIATED CONTENT

Supporting Information

Detailed experimental procedures for the syntheses of polymers and model compounds; additional analytical data, including ¹H NMR spectra of CPEs, GPC, DSC, and TGA data, as well as AFM and optical microscopy images of spin-coated and self-assembled CPE films, additional optical (UV–vis, PL), and IR spectra. This material is available free of charge via the Internet at <http://pubs.acs.org>.

■ AUTHOR INFORMATION

Corresponding Author

*E-mail: scherf@uni-wuppertal.de.

Notes

The authors declare no competing financial interest.

■ ACKNOWLEDGMENTS

Deutsche Forschungsgemeinschaft DFG (grant no. RI 1551/4-1) is gratefully acknowledged for financial support. The research leading to these results has received funding from the European Community's Seventh Framework Programme (FP7/2007-2013) under grant agreement no. 212311 of the ONE-P project. P.G. acknowledges funding by the Emmy-Noether-Programm of the Deutsche Forschungsgemeinschaft DFG.

■ REFERENCES

- (1) Vericat, C.; Vela, M. E.; Benitez, G.; Carro, P.; Salvarezza, R. C. Self-Assembled Monolayers of Thiols and Dithiols on Gold: New Challenges for a Well-Known System. *Chem. Soc. Rev.* **2010**, *39*, 1805–1834.
- (2) Wang, Y.; Zhou, Y.; Sokolov, J.; Rigas, B.; Levon, K.; Rafailovich, M. A Potentiometric Protein Sensor Built with Surface Molecular Imprinting Method. *Biosens. Bioelectron.* **2008**, *24*, 162–166.
- (3) Rusu, P. C.; Brocks, G. Surface Dipoles and Work Functions of Alkylthiolates and Fluorinated Alkylthiolates on Au(111). *J. Chem. Phys. B* **2006**, *110*, 22628–22634.
- (4) Kind, M.; Wöll, C. Organic Surfaces Exposed by Self-Assembled Organothiol Monolayers: Preparation, Characterization, and Application. *Prog. Surf. Sci.* **2009**, *84*, 230–278.
- (5) Roy, D.; Fendler, J. Reflection and Absorption Techniques for Optical Characterization of Chemically Assembled Nanomaterials. *Adv. Mater.* **2004**, *16*, 479–508.
- (6) Zotti, G.; Vercelli, B. Gold Nanoparticles Linked by Pyrrole- and Thiophene-Based Thiols. Electrochemical, Optical, and Conductive Properties. *Chem. Mater.* **2008**, *20*, 397–412.
- (7) Scherf, U.; Adamczyk, S.; Gutacker, A.; Koenen, N. All-Conjugated, Rod–Rod Block Copolymers-Generation and Self-Assembly Properties. *Macromol. Rapid Commun.* **2009**, *30*, 1059–1065.
- (8) Gutacker, A.; Adamczyk, S.; Helfer, A.; Garner, L. E.; Evans, R. C.; Fonseca, S. M.; Knaapila, M.; Bazan, G. C.; Burrows, H. D.; Scherf, U. All-Conjugated Polyelectrolyte Block Copolymers. *J. Mater. Chem.* **2010**, *20*, 1423–1430.
- (9) Zhai, L.; McCullough, R. D. Layer-by-Layer Assembly of Polythiophene. *Adv. Mater.* **2002**, *14*, 901–905.
- (10) Scherf, U.; Evans, R. C.; Gutacker, A.; Bazan, G. C. All-Conjugated Rod–Rod Diblock Copolymers Containing Conjugated Polyelectrolyte Blocks. In *Conjugated Polyelectrolytes: Fundamentals and Applications*; Liu, B., Bazan, G. C., Eds.; Wiley-VCH: Weinheim, Germany, 2013; pp 65–90.
- (11) Distler, H. The Chemistry of Bunte Salts. *Angew. Chem., Int. Ed. Engl.* **1967**, *6*, 544–553.
- (12) Weiss, U.; Sokol, S. *N*-Arylamides of Mercaptoacetic Acid. *J. Am. Chem. Soc.* **1950**, *72*, 1687–1689.
- (13) El-Hewehi, Z.; Taeger, E. Notiz über Bunte-Salze. *J. Prakt. Chem.* **1958**, *191*–195.
- (14) Lecher, H. Z.; Hardy, E. M. Some New Methods for Preparing Bunte Salts. *J. Org. Chem.* **1955**, *20*, 475–487.
- (15) Swan, J. M. Thiols, Disulphides, and Thiosulphates: Some New Reactions and Possibilities in Peptide and Protein Chemistry. *Nature* **1957**, *180*, 643–645.
- (16) Scharsich, C.; Lohwasser, R. H.; Sommer, M.; Asawapirom, U.; Scherf, U.; Thelakkat, M.; Neher, D.; Köhler, A. Control of Aggregate Formation in Poly(3-hexylthiophene) by Solvent, Molecular Weight, and Synthetic Method. *J. Polym. Sci., Part B: Polym. Phys.* **2012**, *50*, 442–453.
- (17) Brown, P. J.; Thomas, D. S.; Köhler, A.; Wilson, J. S.; Kim, J.-S.; Ramsdale, C. M.; Siringhaus, H.; Friend, R. H. Effect of Interchain

Interactions on the Absorption and Emission of Poly(3-hexylthiophene). *Phys. Rev. B* **2003**, *67*, 064203(1–16).

(18) Mai, C.-K.; Zhou, H.; Zhang, Y.; Henson, Z. B.; Nguyen, T.-Q.; Heeger, A. J.; Bazan, G. C. Facile Doping of Anionic Narrow-Band-Gap Conjugated Polyelectrolytes During Dialysis. *Angew. Chem., Int. Ed.* **2013**, *52*, 12874–12878.

(19) Castner, D. G.; Hinds, K.; Grainger, D. W. X-ray Photoelectron Spectroscopy Sulfur 2p Study of Organic Thiol and Disulfide Binding Interactions with Gold Surfaces. *Langmuir* **1996**, *12*, 5083–5086.

(20) Kirihaata, H.; Uda, M. Externally Quenched Air Counter for Low-Energy Electron Emission Measurements. *Rev. Sci. Instrum.* **1981**, *52*, 68–70.

(21) Zhou, X.-H.; Yan, J.-C.; Pei, J. Exploiting an Imidazole-Functionalized Polyfluorene Derivative as a Chemosensory Material. *Macromolecules* **2004**, *37*, 7078–7080.

(22) Yang, R.; Wu, H.; Cao, Y.; Bazan, G. C. Control of Cationic Conjugated Polymer Performance in Light Emitting Diodes by Choice of Counterion. *J. Am. Chem. Soc.* **2006**, *128*, 14422–14423.

(23) Tu, G.; Li, H.; Forster, M.; Heiderhoff, R.; Balk, L. J.; Sigel, R.; Scherf, U. Amphiphilic Conjugated Block Copolymers: Synthesis and Solvent-Selective Photoluminescence Quenching. *Small* **2007**, *3*, 1001–1006.

(24) *Polyfluorenes*; Scherf, U., Neher, D., Eds.; *Advances in Polymer Science*; Springer: Berlin, Heidelberg, 2008; Vol. 212.

(25) Blouin, N.; Michaud, A.; Leclerc, M. A Low-Bandgap Poly(2,7-Carbazole) Derivative for Use in High-Performance Solar Cells. *M. Adv. Mater.* **2007**, *19*, 2295–2300.

(26) Park, S. H.; Roy, A.; Beaupré, S.; Cho, S.; Coates, N.; Moon, J. S.; Moses, D.; Leclerc, M.; Lee, K.; Heeger, A. J. Bulk Heterojunction Solar Cells with Internal Quantum Efficiency Approaching 100%. *Nat. Photonics* **2009**, *3*, 297–303.

(27) Meyer, J.; Hamwi, S.; Kröger, M.; Kowalsky, W.; Riedl, T.; Kahn, A. Transition Metal Oxides for Organic Electronics: Energetics, Device Physics and Applications. *Adv. Mater.* **2012**, *24*, 5408–5427.

(28) Kröger, M.; Hamwi, S.; Meyer, J.; Riedl, T.; Kowalsky, W.; Kahn, A. Role of the Deep-Lying Electronic States of MoO₃ in the Enhancement of Hole-Injection in Organic Thin Films. *Appl. Phys. Lett.* **2009**, *95*, 123301.

(29) Blouin, N.; Michaud, A.; Gendron, D.; Wakim, S.; Blair, E.; Neagu-Plesu, R.; Belletête, M.; Durocher, G.; Tao, Y.; Leclerc, M. Toward a Rational Design of Poly(2,7-Carbazole) Derivatives for Solar Cells. *J. Am. Chem. Soc.* **2008**, *130*, 732–742.

(30) Seo, J. H.; Cho, S.; Leclerc, M.; Heeger, A. J. Energy Level Alignments at Poly[*N*-9''-hepta-decanyl-2,7-carbazole-alt-5,5-(4',7'-di-2-thienyl-2',1',3'-benzothiadiazole)] on Metal and Polymer Interfaces. *Chem. Phys. Lett.* **2011**, *503*, 101–104.

(31) Petri, D. F. S.; Choi, S. W.; Beyer, H.; Schimmel, T.; Bruns, M.; Wenz, G. Synthesis of a Cellulose Thiosulfate and Its Immobilization on Gold Surfaces. *Polymer* **1999**, *40*, 1593–1601.

(32) Wildöer, J. W. G.; Venema, L. C.; Rinzler, A. G.; Smalley, R. E.; Dekker, C. Electronic Structure of Atomically Resolved Carbon Nanotubes. *Nature* **1998**, *391*, 59–62.

(33) Pellegrino, O.; Rei Vilar, M.; Horowitz, G.; Botelho do Rego, A. M. Oligothiophene Films under Electron Irradiation: Electron Mobility and Contact Potentials. *Mater. Sci. Eng., C* **2002**, *22*, 367–372.